Achieving exceedingly constructional characterization of magnesia-yttria (MgO-Y2O3) nanocomposite obtained via oxalate precursor strategy

Ali Omar Turky, Ahmed Esmail Shalan, Emad M.M. Ewais, Hailei Zhao, Mohamed Rashad, Mikhael Bechelany

Achieving Exceedingly Constructional Characterization of Magnesia-Yttria Oxide (MgO-Y_2O_3) Nanocomposite Obtained via Oxalate Precursor Technique

Ali Omar Turky[1,2,3*], Ahmed Esmail Shalan[1], Emad M. M. Ewais[4], Mohamed M. Rashad[1] and Mikhael Bechelany[3]

[1] Electronic & Magnetic Materials Division, Central Metallurgical Research and Development Institute. P.O. 87 Helwan, 11421 Cairo, Egypt.
[2] Center of Excellence in Materials Research for Energy Applications, Central Metallurgical Research and Development Institute. P.O. 87 Helwan, 11421 Cairo, Egypt
[3] Institut Européen des Membranes, IEM – UMR 5635, ENSCM, CNRS, University of Montpellier, Montpellier, France
[4] Refractory & Ceramic Materials Division, Central Metallurgical Research and Development Institute. P.O. 87 Helwan, 11421 Cairo, Egypt.

Corresponding author: (A.O.T.) E-mail: ali_omar155@yahoo.com

Abstract

Magnesium yttrium oxide ($MgO–Y_2O_3$) nanocomposite was prepared through the oxalate precursor method. The broad applications of magnesia composed with yttria in electro-ceramic systems make it particularly remarkable as anode material for solid oxide fuel cells (SOFC). Here oxalate precursor method was used to yield magnesium yttrium oxide nanocomposite with different ratios between magnesium and yttrium (20:80%), (50:50%) and (80:20%) of Mg^{+2}:Y^{+2} ions, respectively. Furthermore, in this paper, the effect of annealing temperature and Mg^{+2}:Y^{+2} ratios on the crystal structure, crystallite size, phase composition, microstructure and optical characteristics were methodically investigated. X-ray Diffraction (XRD) was used to investigate the different phases of magnesium yttrium oxide nanocomposite. Moreover, the field emission scanning electron microscopy (FESEM) showed that the produced powders have the cubic shape like structure with fine grain sizes of 10-150 nm. The spectral characteristic of the produced powders were checked using UV-VIS-NIR-scanning and the obtained results show that these powders have height transmittance bands. Subsequently, the band gap energy for the produced nanocomposites materials was calculated for different Mg^{+2} content and founded to be 4.83 eV, 5.1 eV and 5.08 eV for (20:80), (50:50) and (80:20) % ratios, respectively. From the standpoint of application research, our currently studies consider to be an important achievement to investigate and recognize the features of the MgO-Y_2O_3 system for different applications such as microwave systems, advanced displays (Field Emission Display, Plasma Display, Electroluminescent Display), ultra-fast sensors, durable, infrared windows and lasers.

Keywords: MgO, Y_2O_3, nanocomposite, organic acid precursor, optical properties

Introduction

Materials consist of magnesium ions are consider as a perfect candidates for different applications such as reducing of greenhouse gas emission because of their lightweight and low cost attainable. These advantages enable magnesium materials to replace conventional steel in passenger vehicles with internal combustion engines and reduce consumption inside the vehicles to control the greenhouse gas emissions. The very low density of magnesium makes it a viable material for light-weighting given that it is lighter than aluminium by one-third and steel by three-fourth. Despite these advantages, magnesium materials have certain drawbacks like low elastic modulus and ductility. The disadvantages of these materials can be circumvented with composite technology by incorporating other different materials in the composition of magnesium samples [1, 2].

Many efforts have been performed in order to obtain these Mg based nanocomposite powders using ease ways and with extremely high yield [3-5]. Lately, different types of particulates (metals and ceramic) with different length scales were fabricated [6–12]. Particulate reinforcement in nano length scales, such as alumina and yttrium, has shown the potential to enhance the amalgamation of tensile strengths as well as ductility of MgO powder [3, 4, 12]. Besides, it was very important issue to have a deep look inside not only the structure of the magnesium materials itself but also to understand the composition of it. Further, It is very essential to understand the deformation that occurs during the formation of nanocomposites between magnesium and other metal ions with different types and reinforcements.

There were few studies concern about the properties and features of magnesium-based nanocomposites, although many studies take apart for tailoring the features of magnesium materials. Limited studies exist only on unreinforced magnesium alloys such as AZ31, AZ31B, and AZ91 alloys, which consist of different metals in their composition but the main content is magnesium ions [13-16]. Recently, a Yttrium oxide (Y_2O_3) has attracted attention as a material with outstanding spectral features having large range of promising applications [17]. It is than very important to combine the properties of these two amazing materials in order to obtain new class of composites with outstanding performance. MgO-Y_2O_3 nanocomposite materials were achieved with superb mid-infrared transparency and enhanced mechanical features to be used as infrared window materials [18]. They consolidate the raw materials from

bulk structures through combustion spray pyrolysis process to obtain the desired composite materials. Furthermore, the improvement of the mechanical properties of $MgO\text{-}Y_2O_3$ nanocomposite ceramic materials could be attained by limiting the phase domain size at the nanoscale. This phenomenon is also important to minimize the light scattering at the two-phase grain boundaries [19].

In the current study, we develop for the first time a new class of $MgO\text{-}Y_2O_3$ nanocomposite with different molar ratios using ease wet chemical technique. We depict incipient perception on the structure and the features of the nanocomposite-grained materials and describe the fabrication of three different $MgO\text{-}Y_2O_3$ nanocomposites with various molar composition contents of MgO (20, 50 and 80 mol, % of Mg) using organic acid precursor method. The phase detection, structure morphology and optical features of the as-prepared materials were investigated.

Experimental Section

Chemicals and Materials

All the chemicals used in this study such as magnesium chloride hexahydrate ($MgCl_26H_2O$, CAS: 7791-18-6, 99.0%, Merck), yttrium nitrate hexahydrate, (CAS: 13494-98-9, 99.9% metals basis (, Sigma Aldrich) and oxalic acid as source of organic acid (CAS: 6153-56-6, organic 98%, Sigma Aldrich) were of analytical stage and incorporated in the work without further purification. Deionized water was used in every step of the experiments.

Stoichiometry Control Procedures to Prepare $MgO\text{-}Y_2O_3$ Nanocomposite Materials

Magnesium yttrium oxide ($MgO\text{-}Y_2O_3$) powders were obtained using aqueous solutions of magnesium chloride hexahydrate and yttrium nitrate hexahydrate with different molar ratios (20, 50 and 80 %). Oxalic acid concerning with the stoichiometric ratios of (Mg^{+2} and Y^{+2}) was dropped to the solution to follow the organic acid precursor method as mentioned elsewhere [20-22]. Stirring of the formed solution was gently occurred and then evaporated at 80°C till a clear, viscous gel was obtained. After that, the gel was dried at 110 °C for 24 h. The dry precursors were

heated at a rate of 10 °C/min in static air at maximum temperatures of 600 °C where they were maintained for 2 h.

Chemical and Physical Characterizations

Bruker AXS diffractometer (D8-ADVANCE Germany) with Cu Kα (λ = 1.54056 Å) radiation, operating at 40 kV and 40 mA was used to check the X-ray powder diffraction (XRD) peaks of the prepared samples. The diffraction data were recorded for 2θ values between 10° and 80° and the scanning rate was 3° min^{-1} (or 0.02°/0.4 s). Field emission scanning electron microscopy (FESEM) was investigated by a JEOL-JSM-5410 (Japan). In addition, Transmission electron microscopy (TEM) was recorded with a JEOL-JEM-1230 microscope, Japan. The UV-Vis absorption spectrum was measured by UV-VIS-NIR-scanning spectrophotometer (jasco-V-570 spectrophotometer, Japan) using a 1 cm path length quartz cell. The formed magnesium yttrium oxide nanostructure powders were ultrasonicated in deionized water to yield homogeneous dispersion. In addition, pure distilled water solution was used as a blank for the measurements. Finally, Fourier transformer infrared absorption spectrum (FTIR) measurements were achieved using JASCO 3600 spectrophotometer in the wavenumber range (500–4000 cm^{-1}).

Results and Discussion

Phases and Crystal Structure Analysis

X-ray diffraction (XRD) analysis was used to detect the structure phases of the obtained nanocomposite materials at different molar ratios of Mg^{+2}:Y^{+2} as well as at different annealing temperatures for the prepared samples.

Firstly, we investigate the characterization of the fabricated nanocomposites samples at different contents of Mg^{+2}:Y^{+2} ions. Figure 1a illustrates the formation of as-prepared MgO-Y_2O_3 nanocomposite powders. The obtained planes indicate that the acquired phases of MgO and Y_2O_3 are corresponding to pure cubic phase structure, which correlated to (reference PDF card No. 04-0829) and (reference PDF card No. 05-0574) for MgO and Y_2O_3, respectively [23]. The average grain size calculated from the peak broadening effect using Scherer's formula is ~23.7 nm. Furthermore, the average particle size for the prepared sample at different molar ratios of Mg^{+2} ion are summarized and presented in table 1. We can noticed that the monoclinc Y_2O_3 is

the most prominent phase in the case of the composition of which is Y_2O_3 more rich than magnesium (80 Mol %).

Moreover, after the preparation of the desired nanocomposites, it was necessary to check the optimal annealing temperature to obtain these materials. We have optimized the annealing parameters for the nanocomposite phase of MgO-Y_2O_3 and founded that annealing the obtained powder at 600^{o}C for 2h can resulted with the proposed phase. While, by rising the temperature to 800 or 1000^{o}C, a decomposition for the nanocomposite occurs and we can notice the formation of the separate MgO and Y_2O_3 phases as illustrated in Figure 1 (b). Besides, at low temperature, i.e. 200 and 400 ^{o}C, (results not shown here), the obtained materials were amorphous. All of the above can conclude that 600^{o}C is the best temperature factor to attain magnesium-yttrium oxide nanocomposite structure in crystalline and coveted form.

Micro and Morphological Structure Characterization

FESEM micrographs show a single-phase structure for (80:20) and (50:50) Mg:Y samples, while, secondary-phase particles with dark contrast can be observed by increasing the percentage of Y^{+2} in (20:80) Mg^{+2}:Y^{+2}. The obtained typical micrographs can confirm the formation of composite with different molar ratios at nano-scale range. At molar ratio of 20% magnesium, an agglomeration appeared plainly for the obtained particles in the nanocomposites structure. By increasing the molar ratio of magnesium to 50 %, the materials appeared as cubic like structure, while at 80 % magnesium, the homogeneity of the material is increased and the morphology appeared as a cubic structure. The apportionment of grain size also becomes more homogeneous as shown in Figure 2 (a-c). The obtained micrographs illustrate the allocation of nano-yttria particulates in magnesium matrix obtained at different molar ratios of Mg^{+2}:Y^{+2}. When the grain size of the large amount of magnesium is compared to that of magnesium nanocomposites at different molar ratios with yttrium, average grain size was smaller in case of high amount of yttrium substituted than that in the low amount samples. The shaped phases as well as the different average sizes of the obtained powders at different molar ratios of Mg^{+2}:Y^{+2} are summarized in Table 1. Moreover, the average particle size founded to be 12.8 nm for 20% Mg^{+2}, 23.7 nm for 50% Mg^{+2} and 20.5 nm for 80% Mg^{+2}, respectively. It is founded that, the shape morphology of magnesium yttrium oxide nanocomposite is

transformed from the cubic shape to the monoclinic shape according to the effect of the Y^{+2} ion content.

To investigate more in details the obtained nanocomposite ceramic powders, TEM studies at different magnifications were investigated. The microstructures and phase distributions of magnesia-yttria nanocomposites obtained from the treated powder were homogeneous. The microstructure of MgO-Y_2O_3 series are conducted by TEM as shown in Fig. 3 (a-c) for (80:20), (50:50) and (20:80) of Mg^{+2}:Y^{+2}, respectively. No free grain size of MgO or Y_2O_3 can be founded which confirm the presence of intercalated nanocomposite structure. The spinel grain shape is angular and spatial distribution of the various phases pores are mainly present in the intergranular structure. Fig. 3b shows the micrograph of the 50 wt. % Y_2O_3 and 50 wt.% MgO. Y ions have entered in the spinel grains and it observed as white shinny dots on the grains. The lattice strain generated by replacement of Mg^{+2} by Y^{3+} ion has enhanced the mass transfer, resulting higher densification and increased grain size to almost 50 nm. The nature of the prepared MgO 80 Wt % : Y_2O_3 20 Wt % grains was highly compact and angular as indicated from the obtained results. The average grain size is 35 nm, which is much higher comparing to the other samples. In addition, further studies have been carried out for the obtained nanocomposite powder samples to check the morphology of these powders at low magnification and to confirm the crystallinity behavior as shown in Figure 3 (d-f) for (80:20), (50:50) and (20:80) of Mg^{+2}:Y^{+2}, respectively. The results confirm the formation of MgO-Y_2O_3 nanocomposites at different molar ratios of Mg^{+2}:Y^{+2} due to the existence of different particles composition integrated with each other in the obtained images. Hence, the low magnification images can generate better insights into the fabricated nanocomposite microstructures.

Optical and Spectral Properties

Figure 4 shows the transmittance spectra of MgO-Y_2O_3 powder obtained by organic acid precursors method produced at calcinations temperature of 600 ^oC for 2 h with different molar ratios of Mg:Y ions content (20:80-50:50-80:20). The investigated spectra were obtained for the samples at the wavelength range from 200-800 nm. Despite all the materials spectrum have the same nature, the degree of transmission was related to the crystallite size of each one. The results confirm the

existence of transparent layers as the curve has a maximum peak at ~ 90% at about 300 nm. In addition, the transmittance spectra showed band-edge absorptions for all samples in the range of 200–300 nm. The band-edge absorption is shifted to lower wavelength with the increasing of the yttrium molar ratios. In addition, the obtained results confirmed that by increasing the yttrium amount in the composite, the band gap shifted to the lower wavelength with higher energy induced a red shift behavior.

The band gap energy of the obtained materials can be calculated and platted as shown in Figure 5. Furthermore, MgO-Y_2O_3 nanocomposite samples that obtained by oxalate precursors method show compressive stress relaxation which is due to the inter band transition associated with surface ions five-fold coordination in the matrixes. We can notice that the energy value in all the obtained nanocomposite with different molar ratios of Mg:Y is smaller than the band gap (7.8eV) of bulk MgO. Other absorption bands appeared due to the oxygen vacancy/defect centered in both the bulk and the surface of MgO. In addition, the reduction of energy levels and the increase in the E_g values may be induced by the increase of the structural organization in the nanocomposite structure. Moreover, the change in electronic structure as well as the lattice parameter can confirm the variation in the band gap energy. Subsequently, the oxygen deficiency, the density and the grain size can effect positively on the optical properties. All the above results show that the optical properties of MgO-Y_2O_3 nanocomposite are easily controlled, which indicates that MgO-Y_2O_3 nanocomposite samples are a promising candidate for electro-optic applications [20].

Besides, Figure 6 illustrates the FTIR spectrum of the prepared samples. The existence of H_2O in the magnesium oxalate in the formed compounds can be confirmed through the absorption band around 4000 cm^{-1} which is founded to be abroad and composed of several peaks that is related to –OH-group-stretching vibrations mode. Furthermore, the peaks founded in the range 3100–3700 cm^{-1} were corresponding to the bending mode of –OH group in the obtained samples. The two absorption bands around 2978 and 2851 cm^{-1} are due to surface –OH stretch arising from hydroxyl groups in dissociated state or C–H stretch of organic residue [24]. In our work case, the existence of absorption peak at 1649 cm^{-1} is consider to be an important indicator for chelating with carbonyl group (CQO) and formation of an inorganic ester (i.e., magnesium oxalate). Moreover, the symmetrical and asymmetrical vibration modes of the carbonyl group can be noticed at wavenumbers of 1653 and 1630 cm^{-1}, respectively. The combination of metals like in magnesium

and yttrium oxalate in the presence of $(C_2O_4)_2$ ion can form easily the unionized and uncoordinated COO, which characterized by a single stretching absorption band at 1750–1700 cm^{-1}. In addition, the shift towards lower frequency and splits into two bands which occurred to the absorption peak can be noticed and summarized in figure 6 for the obtained nanocomposite powder materials for the three samples with different molar ratios of Mg^{+2}:Y^{+2} [25]. Subsequently, the existence of $MgC_2O_4.2H_2O$ compound can easily confirmed through the obtained IR absorption peaks. Besides, the formation of (ns (C–O)) as well as (d (OCQO)) modes can be assigned to the absorption peaks at 1371 and 1325 cm^{-1}, respectively. In addition, the weak band at 1118 cm^{-1} corresponds to C–O stretching, while the peak at 688 cm^{-1} is attributed to bending mode of OQCQO and/or liberation of water [26].

Conclusion

MgO-Y_2O_3 nanoparticles were prepared by simple organic precursor method with different Mg ions contents. These ion ratios are divided into the following ratios 20 Mg^{+2} to 80 Y^{+3}, 50 Mg^{+2} to 50 Y^{+2} and 80 Mg^{+2} to 20 Y^{+2}. This ease pathway can create nanocomposite of magnesia-yttria with small nano-sized particles of 10-30 nm. XRD results show that these particles are composed from Cubic MgO and Y_2O_3 phases. The average particles size is changed according to the change in the Mg ion content. By increasing Mg ion content, the average particle size is increased. In addition, FESEM micrographs show that the morphology of magnesium yttrium oxide is swinging between Cubic and monoclinic phases and this due to the change in Mg ion content. When the Mg ion content decreases to 20 %, the phase is changed from cubic to monoclinic. Moreover, the optical properties of these structures were accordingly changed with the evolution of magnesium ion content. By increasing the Mg content, the transmittance value of light is increased. The band gap energy for produced powder was calculated for different Mg^{+2} content and founded to be 4.83 eV for 20 Mg^{+2} to 80 Y^{+2}, 5.1 eV for 50 Mg^{+2} to 50 Y^{+2} and 5.08 eV for 80 Mg^{+2} to 20 Y^{+2}. All of these lineaments founded for magnesia-yttria nanocomposites open the way towards many applications such as microwave systems, advanced displays, infrared windows and lasers

Acknowledgements

It is worth to mention that Dr. A. O. Turky pursue part of this work at CNRS, University of Montpellier, Montpellier, France through fellowship funded by the French government granted. Furthermore, the authors would like to thank the technical services team in CMRDI for their support.

Reference

1. D. J. Lloyd, *Int Mater Rev*., 1994, **39,** 1.

2. A. Evans, C. S. Marchi, A. Mortensen, springer, Kluwer Academic, Dordrecht, 2003, ISBN 978-1-4615-0405-4, DOI:10.1007/978-1-4615-0405-4.

3. C. S. Goh, J. Wei, L. C. Lee, M. Gupta, *Acta Mater*, 2007, **55**, 5115.

4. S. F. Hassan, M. Gupta, *Mater Sci Eng A*, 2005, **392**, 163.

5. W. L. E. Wong, M. Gupta, *Compos Sci Technol*., 2007, **67**, 1541.

6. P. Perez, G. Garces, P. Adeva, *Compos Sci Technol*., 2004, **64**, 145.

7. H. Ferkel, B. L. Mordike, *Mater Sci Eng A*, 2001, **298**, 193.

8. Q. C. Jiang, H. Y. Wang, B. X. Ma, Y. Wang, F. Zhao, *J Alloys Compds*., 2005, **386**, 177.

9. H. Y. Wang, Q. C. Jiang, Y. Wang, B. X. Ma, F. Zhao, *Mater Lett.*, 2004, **58**, 3509.

10. G. Graces, M. Rodriguez, P. Perez, P. Adeva, *Mater Sci Eng A*, 2006, **419**, 357.

11. Z. Xiuqing, W. Haowei, L. Lihua, T. Xinying, M. Naiheng, *Mater Lett*, 2005, **59,** 2105.

12. S. F. Hassan, M. Gupta, *J Alloys Compds*, 2007, **429**, 176.

13. Y. Chen, Q. Wang, J. Peng, C. Zhai, W. Ding, *J Mater Process Technol.*, 2007 **182**, 281.

14. T. Murai, S. Matsuoka, S. Miyamoto, Y. Oki, *J Mater Process Technol.*, 2003, **141**, 207.

15. D. M. Lee, B. K. Suh, B. G. Kim, J. S. Lee, C. H. Lee, *Mater Sci Technol.*, 1997, **13**, 590.

16- K. S. Tun, M. Gupta, *J Mater Sci.*, 2008, **43**, 4503–4511.

17. M. H.-Oghaz, R. S. Razavi, M. Barekat, M. Naderi, S. Malekzadeh, M. Rezazadeh, *J.Sol-Gel Sci. and Tech.*, 2016, **78**, 682–691.

18- T. Stefanik, R. Gentilman, and P. Hogan, *Proc. SPIE*, 2007, **6545**, 65450A1-65450A5.

19-J. Wang, E. H. Jordan, and M. Gell, *Journal of Thermal Spray Technology*, 2010, **19**, 873-878

20. A. O. Turky, A. E. Shalan, M. M. Rashad, H. Zhao, M. Bechelany, *Journal of Materials Science: Materials in Electronics*, 2018, **29**, 14582-14588.

21. A. O. Turky, M. M. Rashad, M. Bechelany, *Materials & Design*, 2016, **90**, 54-59.

22. A. O. Turky, M. M. Rashad, A. M. Hassan, E. M. Elnaggar, M. Bechelany, *Phys. Chem. Chem. Phys.*, 2017, **19**, 6878-6886.

23. I. Khan, N. Musahwar, M. Zulfequar, *Ceramics – Silikáty*, 2010, **54**, 263-268.

24. C. M. Lee, J. D. Kubicki, B. Fan, L. Zhong, M. C. Jarvis, and S. H. Kim, *J. Phys. Chem. B*, 2015, **119**, 15138–15149.

25. O. O. Mesele and W. H. Thompson, *J. Phys. Chem. A*, 2017, **121**, 5823–5833.

26. T. Cao, R. You, X. Zhang, S. Chen, D. Li, Z. Zhang and W. Huang, *Phys. Chem. Chem. Phys.*, 2018, **20**, 9659-9670.

Table (1) show the formation conditions of magnesium yettrium oxide nanoparticles prepaed by oxalate precursor method including the component percentage, ignation tempreture and time as well as averge particle size and phase shape obtained.

Components (%)		**Ignition Temperature ^{o}C /time hr.**	**Average particle size, (nm)**	**Phase shape**	
Mg^{2+}	**Y^{3+}**			**Phase**	**Crystal shape**
50	**50**	600 ^{o}C / 2h	23.7	MgO, Y_2O_3	Cubic
20	**80**	600 ^{o}C / 2h	12.8	Y_2O_3	Monoclinic
80	**20**	600 ^{o}C / 2h	20.5	MgO,Y_2O_3	Cubic

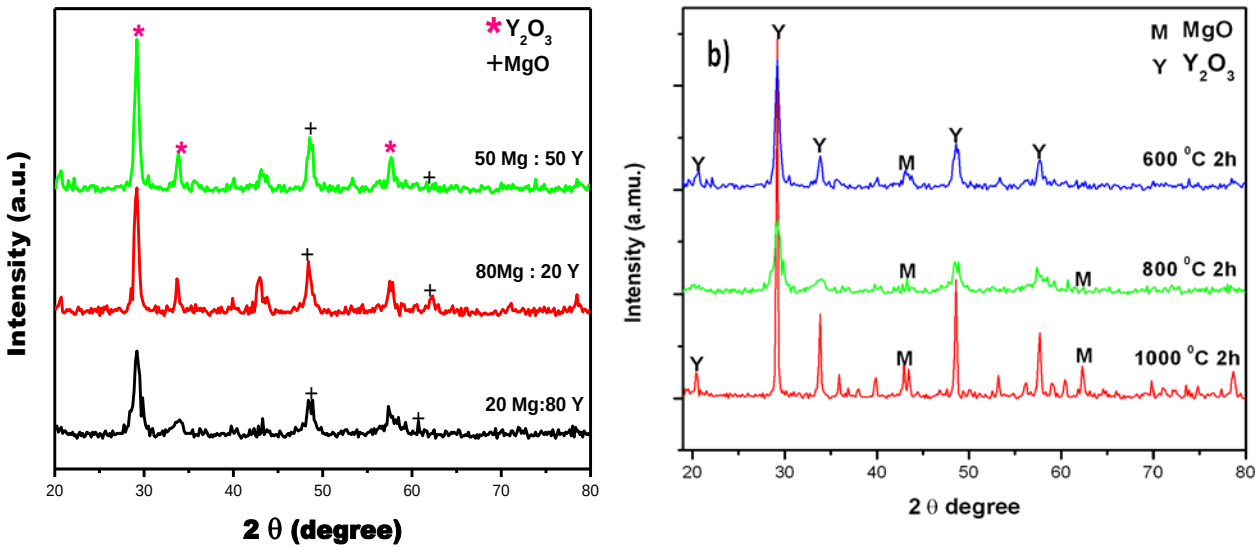

Figure 1: The XRD pattrens of (a) the produced magnesium yettrium oxide nanoparticles at diferent Mg^{+2} ion content annealed at 600 ^{0}C for 2 h and (b) the optimization of annealing parameters for the nanocomposite phase of MgO-Y_2O_3.

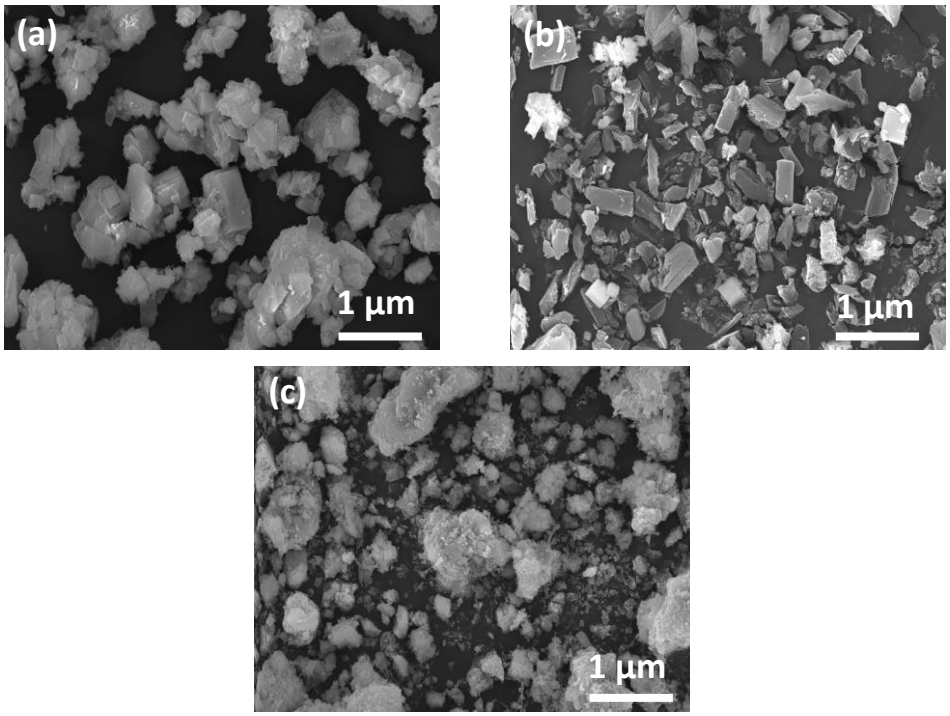

Figure 2: The FESEM images of produced magnesium yettrium oxide nanopowders at diferent Mg^{+2} ion content (a) 80Mg:20Y, (b) 50Mg:50Y and (c) 20Mg:80Y annealed at 600 ^{o}C for 2 h .

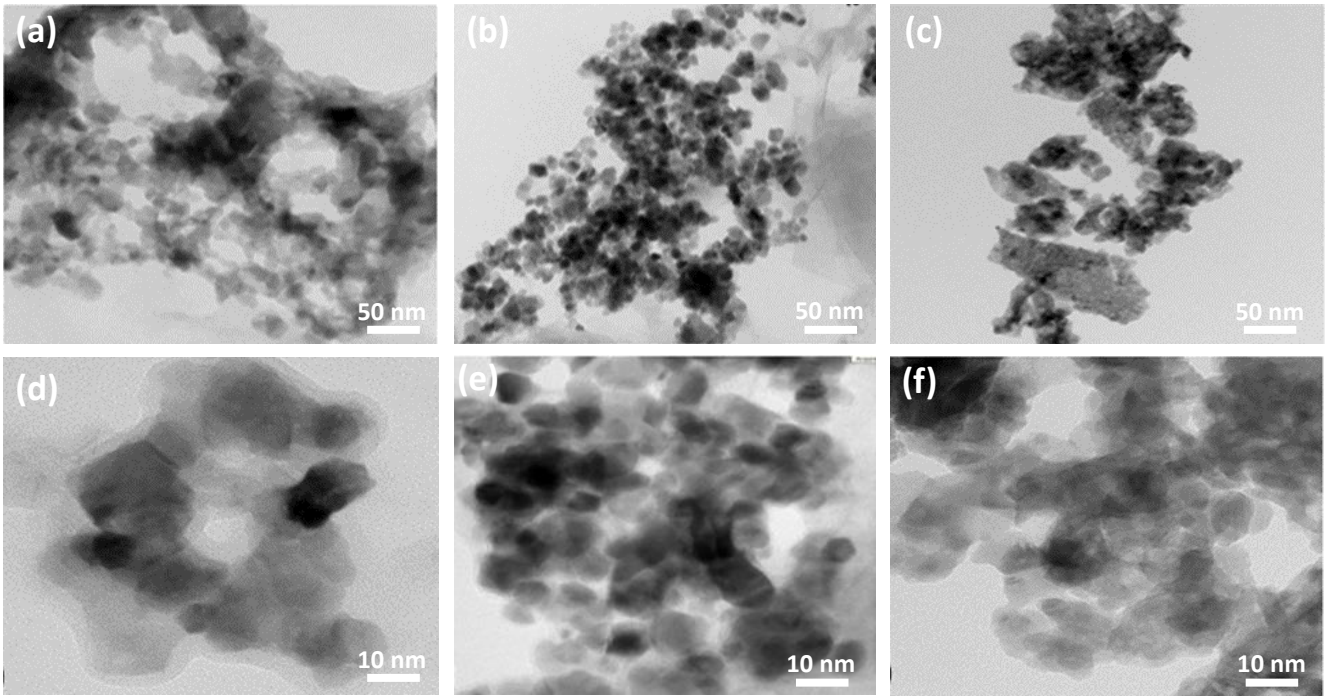

Figure 3: The TEM images at different magnifications of produced magnesium yettrium oxide nanopowders at different Mg^{+2} ion content (a and d) for 80Mg:20Y sample, (b and e) for 50Mg:50Y sample and (c and f) for 20Mg:80Y sample calcined at 600 ^{0}C for 2 h

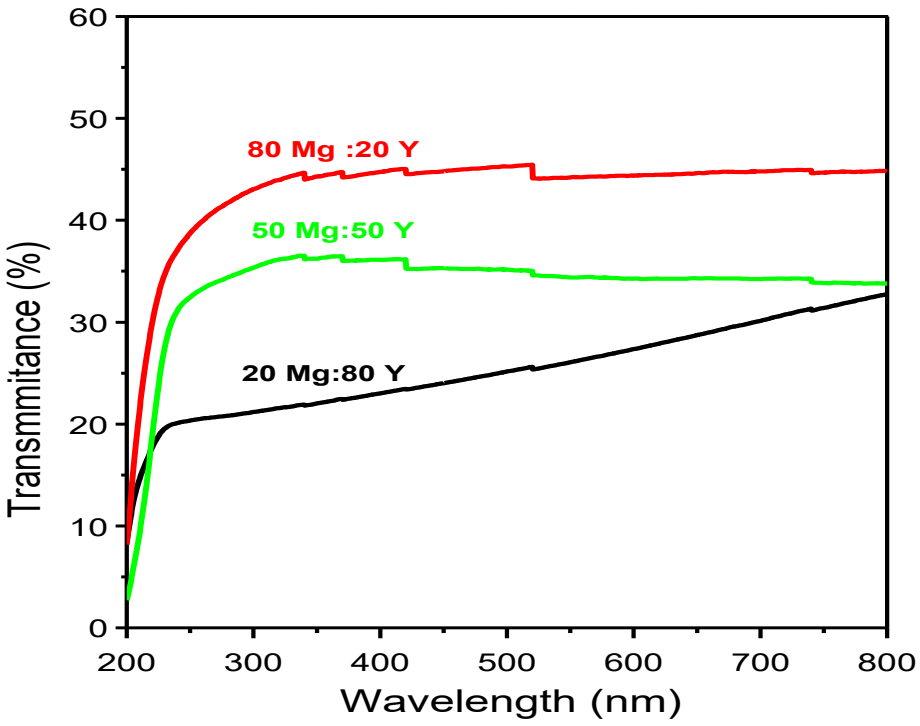

Figure 4: Optical transmittance of the produced magnesium yettrium oxide nanopowders at diiferent Mg^{+2} ion content (a) 20Mg:80Y, (b) 50Mg:50Y and (c) 80 Mg:20Y annealed at 600 ^{0}C for 2 h .

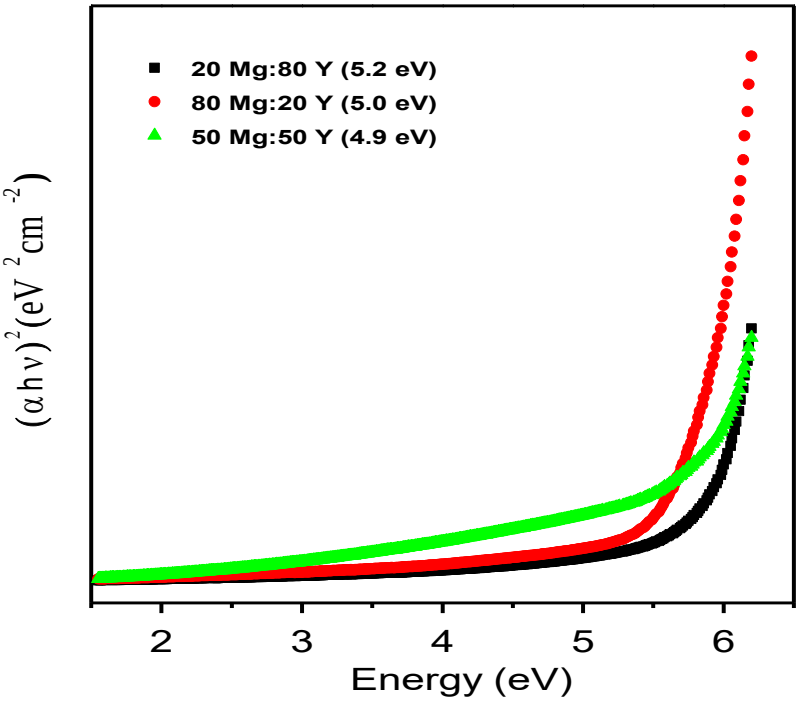

Figure 5: Optical band gap energy of the produced magnesium yettrium oxide nanopowders at diiferent Mg^{+2} ion content (a) 20Mg:80Y, (b) 50Mg:50Y and (c) 80 Mg:20 Y annealed at 600 ^{0}C for 2 h .

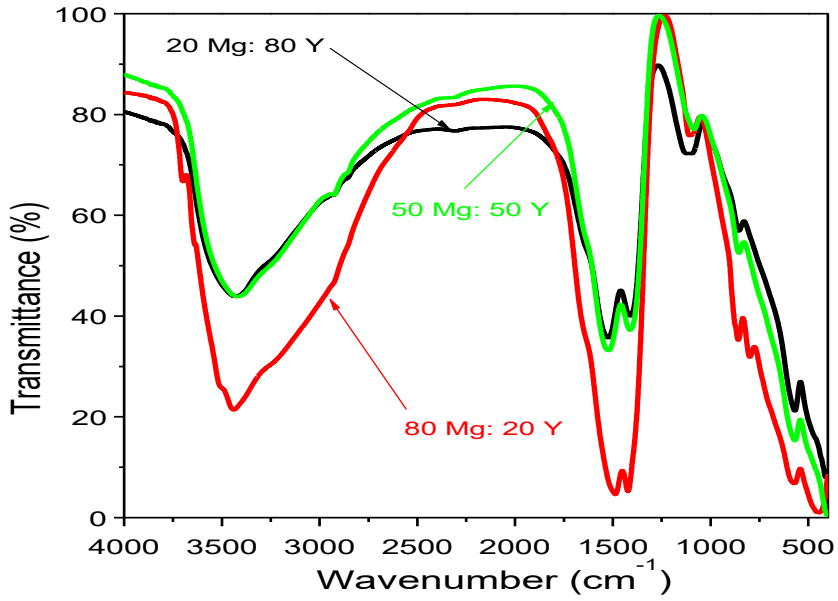

Figure 6: FT-IR spectrum of the produced magnesium yettrium oxide nanopowders at different Mg^{+2} ion content annealed at 600 ^{0}C for 2 h .

Table of content (TOC)